

Predicting Yield Strengths of Noble Metal High Entropy Alloys

Céline Varvenne^{a,*}, William A. Curtin^b

^a*Aix-Marseille Univ.-CNRS, Centre Interdisciplinaire des Nanosciences de Marseille, Campus de Luminy, case 913, Marseille F-13288, France*

^b*EPFL, Laboratory for Multiscale Mechanics Modeling, Lausanne CH-1015, Switzerland*

Abstract

Recent data on the Noble metal (Pd-Pt-Rh-Ir-Au-Ag-Cu-Ni) high entropy alloys (HEAs) shows some of these materials to have impressive mechanical properties. Here, a mechanistic theory for the temperature-, composition-, and strain-rate-dependence of the initial yield strength of fcc HEAs is **applied** to this alloy class, with inputs obtained through “rule-of-mixtures” models for both alloy lattice and elastic constants. Predictions for PdPtRhIrCuNi are in good agreement with **available** experiment and the model provides useful insights into this system. The model is then used to explore other alloy compositions within this broad class **to guide design of new stronger** Noble metal HEAs.

Keywords: High Entropy Alloys, Noble metals, Mechanical properties, Solution Strengthening, Yield stress predictions

High Entropy Alloys (HEAs) are N -component random solid-solution alloys at, typically, equi-concentration $c_n = 1/N$ for each element n . However, there is no restriction to equicomposition, and other compositions are emerging rapidly. Some of these HEAs have remarkable mechanical properties [1, 2, 3, 4], making them a new attractive class of structural materials. While discovery of these materials can be accomplished by direct fabrication of potential compositions, the vast range of possible compositions suggests a high need for theoretical models to predict (i) those compositions that are thermodynamically stable as single-phase solid solutions and (ii) the mechanical properties of the resulting alloys.

The present authors **previously** developed a detailed theory to predict the finite-T, finite-strain-rate initial yield strength of arbitrary random fcc alloys. The theory envisions the random alloy as a high-concentration solute-strengthened alloy in which each elemental component is a “solute” within an “effective-medium matrix” describing the average alloy properties [5, 6]. Strengthening is due to the interactions of dislocations in the effective

matrix with the spatial *concentration fluctuations* in the multi-component random alloy. **The theory predictions have been successfully validated in the family of Ni-Co-Fe-Cr-Mn Cantor alloys [5, 7], to virtual alloys described by embedded-atom-method potentials [5], and to alloys formed by doping the Cantor-type alloys with dilute Al additions [8].**

Here, we apply the theory using estimated rule-of-mixtures-type inputs that enable fully analytic *a priori* predictions to predict strengths in recently-studied Noble metal Pd-Pt-Rh-Ir-Au-Ag-Cu-Ni HEAs [9]. The theory makes quantitative agreement with available experiment, and provides valuable insights into various experimental findings. It is then used to provide directions for optimization of alloy compositions achieving high strengths in this broad class of HEAs.

The full theory is reduced to an analytic model by assuming that individual solutes interact elastically with dislocations in the average alloy matrix. That is, a solute of type n at lattice position (x_i, y_j) , with x_i the position along the glide direction and y_j along the normal to the glide plane, has an interaction energy with respect to a dislocation lying along z given by $U^n(x_i, y_j) = -p(x_i, y_j)\Delta V_n$ where ΔV_n is the misfit volume of the solute n in the *average alloy* matrix and $p(x_i, y_j)$ is the pressure field

*Corresponding author

Email address: varvenne@cinam.univ-mrs.fr (Céline Varvenne)

at (x_i, y_j) generated by the dislocation in the *average alloy* matrix. For fcc dislocations with Shockley partial dissociation distance $d > 1$ nm, the strength and energy barrier for plastic flow are found to be independent of d . The predicted zero-temperature yield stress τ_{y0} and energy barrier ΔE_b for thermally activated flow are then derived to be

$$\tau_{y0} = 0.01785\alpha^{-\frac{1}{3}}\bar{\mu} \left(\frac{1+\bar{\nu}}{1-\bar{\nu}} \right)^{\frac{4}{3}} \left[\frac{\sum_n c_n \Delta V_n^2}{b^6} \right]^{\frac{2}{3}}, \quad (1)$$

$$\Delta E_b = 1.5618\alpha^{\frac{1}{3}}\bar{\mu}b^3 \left(\frac{1+\bar{\nu}}{1-\bar{\nu}} \right)^{\frac{2}{3}} \left[\frac{\sum_n c_n \Delta V_n^2}{b^6} \right]^{\frac{1}{3}}. \quad (2)$$

The elastic constants $\bar{\mu}$ and $\bar{\nu}$ are those for the random alloy at the *specified composition* and temperature T . The numerical coefficients in Eqs. (2) and (1) are a combination of geometrical and dislocation core structure factors, as described in Ref. [5]. The theory involves the dislocation line tension, written as $\Gamma = \alpha\bar{\mu}b^2$ with $\alpha = 0.123$ as estimated in several atomistic simulations and used previously. Within this elasticity-based theory, the role of the dislocation in the effective matrix and of the ‘‘solutes’’ are well separated, with $\sum_n c_n \Delta V_n^2$ describing the average misfit within the concentrated multi-component solid solution, and with the alloy elastic and lattice constants parameterizing the dislocation [6].

At finite temperature T and finite strain-rate $\dot{\epsilon}$, standard thermal activation theory then leads to the predicted yield stress as

$$\tau_y(T, \dot{\epsilon}) = \tau_{y0}(T) \left[1 - \left(\frac{kT}{\Delta E_b(T)} \ln \frac{\dot{\epsilon}_0}{\dot{\epsilon}} \right)^{\frac{2}{3}} \right], \quad (3)$$

where we explicitly indicate that the quantities $\tau_{y0}(T)$ and $\Delta E_b(T)$ are to be computed using the finite-temperature elastic constants $\bar{\mu}(T)$ and $\bar{\nu}(T)$. When $\tau_y(T, \dot{\epsilon})/\tau_{y0}(T) \simeq 0.5$ or lower, the strength decreases more slowly, as $\tau_y(T, \dot{\epsilon}) = \tau_{y0}(T) \exp\left(-\frac{kT}{0.55\Delta E_b(T)} \ln \frac{\dot{\epsilon}_0}{\dot{\epsilon}}\right)$, but for simplicity we use Eq. (3) throughout this paper. The tensile yield stress of an isotropic polycrystalline sample of the alloy is then obtained by multiplying the shear stress by the Taylor factor 3.06.

Application of the above fully-analytic, parameter-free model requires knowledge of the misfit volumes ΔV_n of the elements in the alloy at composition $\{c_n\}$ and the alloy elastic

Table 1: Experimental lattice parameters [9] and isotropic elastic constants [16, 21] of fcc Pt, Pd, Rh, Ir, Ni, Cu, Au, Ag pure materials, at room temperature.

n	a_n (Å)	μ_n (GPa)	ν_n	E_n (GPa)
Pt	3.924	61	0.38	168.4
Pd	3.891	44	0.39	122.3
Rh	3.803	150.4	0.26	379.0
Ir	3.839	210	0.26	529.2
Ni	3.524	76	0.31	199.1
Cu	3.615	48	0.34	128.6
Au	4.078	27	0.44	77.8
Ag	4.085	30	0.37	82.2

constants at the temperature of interest. To continue with a fully-analytic model, we make two additional approximations to obtain the required inputs, as follows. For the misfit volumes ΔV_n , we use Vegard’s law combined with the atomic volumes $V_n = a_n^3/4$ of the fcc pure elements of lattice constants a_n . The atomic volume of the random alloy is thus computed as $\bar{V} = \sum_n c_n V_n$ and the misfit volumes as $\Delta V_n = V_n - \bar{V}$. For the Noble metal systems studied here, where all elements crystallize in an fcc structure at low temperature, and where all elements aside from Ni are non-magnetic, we expect Vegard’s law to work reasonably well. Deviations to Vegard’s law for many binary solid solution alloys within this family of alloys appear small in a range of experiments and first-principles studies [10, 11, 12, 13, 14, 15].

For the alloy elastic constants, we use a rule-of-mixtures based on the elemental (isotropic polycrystalline) elastic constants E_n , μ_n , and ν_n for each element. Specifically, we compute $\bar{E} = \sum_n c_n E_n$ and $\bar{\mu} = \sum_n c_n \mu_n$, and then compute $\bar{\nu} = \bar{E}/2\bar{\mu} - 1$. This model, while not exact, appears reasonable for Pt-Rh, Pt-Ir and Cu-Ni alloys [16, 17, 18], and also for some virtual materials described by EAM-type interatomic potentials [19, 20]. Since the model is fully analytic, and quite simple, the sensitivity of the predictions to the above assumptions is easily studied. Furthermore, experimental data on the elastic constants and lattice constants of real single-phase alloys can be used in place of the above estimates whenever such data is available.

We now use the above model to make predictions for alloys in the Pd-Pt-Rh-Ir-Au-Ag-Cu-Ni family, which have been fabricated and studied just re-

Table 2: Predicted lattice parameters, isotropic elastic constants (\bar{a} , $\bar{\mu}$, $\bar{\nu}$, \bar{E}), misfit parameter δ , and yield strength $\sigma_y(300\text{ K})$ for various fcc solid solution alloys in the Pd-Pt-Rh-Ir-Cu-Ni-Au-Ag family. Lattice and elastic constants for alloys are computed using the data for pure elements given in Table 1, and as described in the main text. **The typical uncertainty associated with experimental bulk uniaxial tensile strength measurements is ± 15 MPa.**

Alloy	ageing	phase	\bar{a} (Å)	$\bar{\mu}$ (GPa)	$\bar{\nu}$	\bar{E} (GPa)	δ	$\sigma_y(300\text{ K})$ (MPa)	
								pred.	exp.
PdPtRhIrCuNi	as-cast	<i>average</i>	3.772	98.2	0.295	254.4	3.9	561	527
		dendritic	3.794	134.7	0.276	343.8	3.2	587	
		interdendritic	3.763	80.5	0.312	211.1	4.2	521	
	1273 K	dendritic	3.785	126.4	0.279	323.2	3.5	617	
		interdendritic	3.764	80.9	0.311	212.0	4.1	504	
	1473 K	dendritic	3.782	126.8	0.279	324.3	3.5	623	
		interdendritic	3.772	91.6	0.300	238.2	3.9	533	
	1673 K	dendritic	3.795	132.5	0.277	338.2	3.2	578	
		interdendritic	3.762	66.1	0.330	175.9	4.2	423	
AuPdAgPt			3.996	40.5	0.391	112.7	2.2	85	
AuPdAg			4.020	34.6	0.397	94.1	2.2	60	
AuPd			3.987	35.5	0.409	100.0	2.3	80	
Au ₈₀ Ni ₂₀			3.979	36.8	0.386	102.0	5.6	332	
Au ₆₀ Ag ₃₂ Ni ₂₀			4.041	31.8	0.394	88.9	3.7	127	
CuNiRhIr			3.700	121.1	0.276	309.0	3.5	603	

cently [9]. Table 1 provides the standard lattice and elastic constants used for each elemental component at room temperature [9, 16, 21]. Table 2 shows the predicted lattice constants, elastic constants, and key misfit quantity $\sum_n c_n \Delta V_n^2$. The latter quantity is very closely related to the standard δ -parameter $\delta = \sqrt{\sum_n c_n (1 - a_n/\bar{a})^2}$ widely used to characterize multicomponent random alloys where a_n is the lattice constant of element n . When all alloy elements crystallize in the same structure and Vegard's law is applied to the lattice parameter, $\bar{a} = \sum_n c_n a_n$, then $\sum_n c_n \Delta V_n^2$ and δ can be related as $\delta = \sqrt{2 \sum_n c_n \Delta V_n^2 / 9b^6}$. For the present alloys, the difference between these is within $\pm 0.1\%$ for the alloys studied here, and so we use the familiar δ parameter in the following discussion.

Table 2 shows the predicted uniaxial yield stress (tension or compression) at the experimental testing conditions of $T = 300\text{ K}$ and strain rate $\dot{\epsilon} = 10^{-4}\text{ s}^{-1}$ for each alloy considered here. The yield stress was reported **on a single sample of the PdPtRhIrCuNi HEA as shown in Table 2, and agreement between theory and this one experiment is very good (within 6%), especially noting that there are no adjustable parameters in the prediction, and that we use the reduced, elasticity-based, version**

of the theory[5]. While only one experimental data point is available, the sample-to-sample variations in initial yield stress in bulk polycrystalline alloys is usually rather small, for instance ± 15 MPa in the NiCoCrFeMn Cantor alloy that has comparable yield stress 400-600 MPa. VERIF The high strength in the PdPtRhIrCuNi alloy emerges because this material has (i) a large size difference between (Pd, Pt, Rh, Ir) and (Cu, Ni), respectively, making this composition like a pseudo-binary (PdPtRhIr)₂(CuNi)₁ and (ii) a high shear modulus due to the contributions from Ir and Rh.

The as-fabricated PdPtRhIrCuNi material was found experimentally to be a single fcc phase according to X-ray analysis. However, it actually consists of a dendritic phase of composition Pd₈Pt₁₃Rh₂₆Ir₃₄Cu₆Ni₁₃ and an interdendritic phase of composition Pd₂₀Pt₂₁Rh₁₃Ir₇Cu₁₈Ni₂₁ [9]. The predicted lattice constants, elastic constants, and strengths of these two compositions are also shown in Table 2. The lattice constants are very close (misfit of 0.8%), consistent with X-ray analysis and thus supporting the concept of a fully-coherent microstructure. These two compositions can be viewed as pseudo binaries (Pd-Pt-Rh-Ir)₈₁(Cu-Ni)₁₉ (larger $\bar{\mu} = 134$ GPa, smaller $\delta = 3.2\%$) and (Pd-Pt-Rh-Ir)₆₁(Cu-Ni)₃₉ (smaller

$\bar{\mu} = 80.5$ GPa, larger $\delta = 4.2\%$), respectively. Since strength is a combination of $\bar{\mu}$ and δ , the predicted yield stresses are then fairly similar (587 MPa and 521 MPa) and closely bracket that of the predicted hypothetical single-phase alloy (561 MPa). **The theory thus rationalizes why the PdPtRhIrCuNi material consisting of two coherent fcc phases can behave essentially like a single-phase material: dislocations can move coherently through both phases with limited difference in critical resolved shear stress.**

The PdPtRhIrCuNi material was also subjected to heat treatments, during which the compositions of the dendritic and interdendritic phases evolve toward the overall equicomposition phase. The theory makes predictions for the strengths of these phases as well. According to the compositions given in the Supplementary Material of Ref. [9], the predicted lattice constants, elastic constants, and strengths for the various heat treatments are shown in Table 2. The changes in strength are modest, but the theory predicts that heat treatment at 1473 K should yield a slightly stronger material if the volume fractions remain the same. The theory also indicates that heat treatment at 1673 K leads to a significant strength loss in the second phase, which is also becoming the dominant phase. **These predictions await experimental validation.** An interesting possibility from this analysis is that as-cast HEAs that form two coherent phases could be “heat-treatable” to improve strength.

Based on the success of the simplified theory, the theory can be used to predict strengths of other HEAs in this family of alloys and therefore enables *a priori* search/design for stronger HEAs within this family. The theory predicts that the strengths for multinary alloys that do not contain the smallest atoms (Ni, Cu) are reduced significantly. For instance, as shown in Table 2, AuPdAgPt has a predicted strength of only $\sigma_y = 85$ MPa since the misfit is small (a pseudo-binary of (PtPd)(AuAg) with modest size difference) and the elastic modulus is low ($\bar{\mu} = 40.5$ GPa) due to the absence of Rh and Ir. Similar reduced strengths are obtained for AuPd and AuPdAg equiatomic alloys. In general, the theory predicts that the strongest possible alloys are equi-binary alloys of the largest and smallest atoms (to maximize the misfit parameter) and/or systems with smaller misfit parameter but larger moduli. Thus, as indicated in Table 2, a hypothetical fcc solid solution AuNi alloy (not thermodynamically stable at 300 K) is pre-

dicted to have a strength of $\sigma_y = 780$ MPa while a hypothetical solid-solution IrNi alloy is predicted to have a strength of $\sigma_y = 984$ MPa. With the data in Table 1, the theory predicts the strengths for other solid-solution fcc alloys, such as Au₈₀Ni₂₀ ($\sigma_y = 332$ MPa) developed for hard contact applications [12] and 18-kt Au₆₀Ag₃₂Ni₈ [22] in the solid-solution state ($\sigma_y = 127$ MPa). The theory also predicts that the CuNiRhIr alloy will have a high strength of $\sigma_y = 603$ MPa while retaining the 4-component alloy complexity that could facilitate fabrication of a solid solution in the random state.

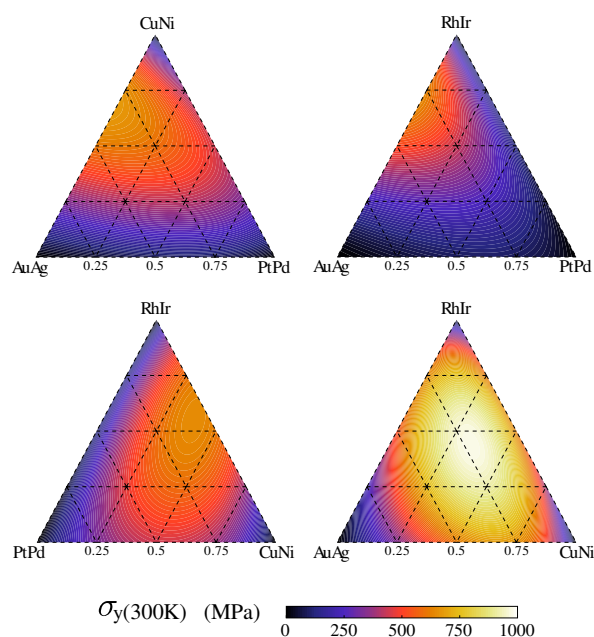


Figure 1: Predicted yield strength σ_y at 300 K for various pseudo-ternary fcc solid solution alloys, containing Au, Ag, Ir, Rh, Cu and/or Ni chemical species.

The present model can be used to extensively sample the full compositional space of this class of alloys to find further alloy compositions with desirable high strengths. As a first step in this direction, Fig. 1 shows examples of such predictions for some - hypothetical 6-component solid solution alloys in the form of pseudo-ternaries, e.g. $(\text{AuAg})_x(\text{PdPt})_y(\text{RhIr})_{1-x-y}$. Such pseudo-ternaries capture the major range of behaviors in a condensed form. Strengths greater than 600 MPa are predicted for the near-pseudo-binary compositions $(\text{AuAg})_{0.4}(\text{CuNi})_{0.6}$, $(\text{AuAg})_{0.3}(\text{RhIr})_{0.7}$, and $(\text{CuNi})_{0.4}(\text{RhIr})_{0.6}$ and in the vicinity of the pseudo-ternary $(\text{AuAg})_{0.24}(\text{CuNi})_{0.38}(\text{RhIr})_{0.38}$.

These alloys are all predicted to be stronger than the PdPtRhIrCuNi studied to date, so are all interesting candidates for possible fabrication while retaining the high complexity of HEAs that may assist in creation of stable fcc solid solutions. A practical integrated optimization process for alloy design should include additional constraints on, for instance, phase stability, cost, and other properties such as corrosion, creep, and oxidation. Nonetheless, the present analytic model for strength, with the elemental material data given above, can be easily used within such a design process by any researchers.

The full fundamental theory is robust: originally developed for dilute solid solution alloys and then extended to finite concentration multi-component alloys, it is has been validated against both experimental measurements and numerical simulations on model HEAs [5, 7, 8, 23, 24]. However, that model requires detailed knowledge of the solute/dislocation interaction energies. The elasticity theory used here and elsewhere [5, 7, 8] assumes that these interactions depend only on misfit volumes, and that neither local disorder near the cores of partial dislocations nor solute/stacking fault interactions are crucial to the strengthening. Related to the partial cores, the model assumes a partial core spreading that is comparable to that found in the Cantor alloys, but this could vary somewhat with the stable/unstable stacking fault energies of the alloy, which are not known in the present systems. As more detailed information (experiment or theory) emerges about the dislocation core structures, refined predictions can be made. The model is also for random alloys, thus implicitly neglecting any short-range order. However, given the quantitative success of the elastic model for a number of real HEA systems, it seems that none of the above effects are significant in determining the overall energetics of the problem. The simplified theory presented here thus provides a *framework*, within a set of reasonable and partially-validated assumptions, for analytic estimates of the initial yield strengths of potential HEAs and, more generally, any multi-component fcc random alloys. This makes the theory an important tool for systematic approaches to the identification of high-performing materials while preserving a solid physical understanding of the origins of the performance.

Acknowledgments

Support for this work was provided through a European Research Council Advanced Grant, “Predictive Computational Metallurgy”, ERC Grant agreement No. 339081 - PreCoMet.

References

- [1] M.-H. Tsai, J.-W. Yeh, High-entropy alloys: A critical review, *Mater. Res. Lett.* 2 (3) (2014) 107–123. doi:10.1080/21663831.2014.912690.
- [2] Y. Zhang, T. T. Zuo, Z. Tang, M. C. Gao, K. A. Dahmen, P. K. Liaw, Z. P. Lu, Microstructures and properties of high-entropy alloys, *Prog. Mater. Sci.* 61 (2014) 1–93. doi:10.1016/j.pmatsci.2013.10.001.
- [3] B. Gludovatz, A. Hohenwarter, D. Catoor, E. H. Chang, E. P. George, R. O. Ritchie, A fracture-resistant high-entropy alloy for cryogenic applications, *Science* 345 (6201) (2014) 1153–1158. doi:10.1126/science.1254581.
- [4] B. Gludovatz, A. Hohenwarter, K. V. S. Thurston, H. Bei, Z. Wu, E. P. George, R. O. Ritchie, Exceptional damage-tolerance of a medium-entropy alloy CrCoNi at cryogenic temperatures, *Nat. Commun.* 7 (2015) 10602. doi:10.1038/ncomms10602.
- [5] C. Varvenne, A. Luque, W. A. Curtin, Theory of solute strengthening for high entropy alloys, *Acta Mater.* 118 (2016) 164–176. doi:10.1016/j.actamat.2016.07.040.
- [6] C. Varvenne, G. P. M. Leyson, M. Ghazisaeidi, W. A. Curtin, Solute strengthening for random alloys, *Acta Mater. Overview* 124 (2017) 660–683. doi:10.1016/j.actamat.2016.09.046.
- [7] G. Laplanche, J. Bonneville, C. Varvenne, W. A. Curtin, E. P. George, Thermal activation parameters for plastic flow reveal deformation mechanisms in the CrMnFeCoNi high-entropy alloy, submitted.
- [8] C. Varvenne, W. A. Curtin, Strengthening of high entropy alloys by dilute solute additions: CoCrFeNiAl_x and CoCrFeNiMnAl_x alloys, *Scr. Mater.* 138 (2017) 92 – 95. doi:https://doi.org/10.1016/j.scriptamat.2017.05.035.
- [9] S. Sohn, Y. Liu, J. Liu, P. Gong, S. Prades-Rodel, A. Blatter, B. E. Scanley, C. C. Broadbridge, J. Schroers, Noble metal high entropy alloys, *Scripta Mater.* 126 (2017) 29 – 32. doi:http://dx.doi.org/10.1016/j.scriptamat.2016.08.017.
- [10] W. Pearson, A handbook of lattice spacings and structures of metals and alloys, Vol. 4 of International Series of Monographs on Metal Physics and Physical Metallurgy, Pergamon, 1958, pp. 1 – 1446. doi:http://dx.doi.org/10.1016/B978-1-4832-1318-7.50009-7.
- [11] G. C. Bond, The electronic structure of platinum-gold alloy particles, *Platinum Metals Rev.* 21 (2) (2007) 63–68. doi:10.1595/147106707X187353.
- [12] Z. Yang, D. J. Lichtenwalner, A. S. Morris, J. Krim, A. I. Kingon, Comparison of Au and Au-Ni alloys as contact materials for mems switches, *J. Microelectromech. Syst.* 18 (2) (2009) 287–295. doi:10.1109/JMEMS.2008.2010850.
- [13] S. Lu, Q.-M. Hu, E. K. Delczeg-Czirjak, B. Johansson, L. Vitos, Determining the minimum grain size in severe plastic deformation process via first-principles

- calculations, *Acta Mater.* 60 (11) (2012) 4506 – 4513. doi:10.1016/j.actamat.2012.04.024.
- [14] S. Porobova, T. Markova, V. Klopotov, A. Klopotov, O. Loskutov, V. Vlasov, Copper-based alloys, crystallographic and crystallochemical parameters of alloys in binary systems Cu-Me (Me=Co, Rh, Ir, Cu, Ag, Au, Ni, Pd, Pt), in: S. Starenchenko, Y. Soloveva, N. Kopanitsa (Eds.), *Advanced Materials in Technology and Construction (AMTC-2015)*, Vol. 1698 of AIP Conference Proceedings, 2016. doi:10.1063/1.4937827.
- [15] A. Leibner, C. Braun, J. Heppe, M. Grewer, R. Birringer, Plastic yielding in nanocrystalline pd-au alloys mimics universal behavior of metallic glasses, *Phys. Rev. B* 91 (2015) 174110. doi:10.1103/PhysRevB.91.174110.
- [16] J. Merker, D. Lupton, M. Toepfer, H. Knake, High temperature mechanical properties of the platinum group metals, elastic properties of platinum, rhodium and iridium and their alloys at high temperatures, *Platinum Metals Rev.* 45 (2) (2001) 74–82.
- [17] S. G. Epstein, O. N. Carlson, The elastic constants of nickel-copper alloy single crystals, *Acta Metall.* 13 (1965) 487–491.
- [18] R. E. Schmunk, C. S. Smith, Elastic constants of copper-nickel alloys, *Acta Metall.* 8 (1960) 396–401.
- [19] S. I. Rao, C. Varvenne, C. Woodward, T. A. Parthasarathy, D. B. Miracle, O. N. Senkov, W. A. Curtin, Atomistic simulations of dislocations in a model BCC multicomponent concentrated solid solution alloy, *Acta Mater.* 125 (2017) 311–320. doi:10.1016/j.actamat.2016.12.011.
- [20] S. Rao, C. Woodward, T. Parthasarathy, O. Senkov, Atomistic simulations of dislocation behavior in a model FCC multicomponent concentrated solid solution alloy, *Acta Mater.* 134 (2017) 188 – 194. doi:http://dx.doi.org/10.1016/j.actamat.2017.05.071.
- [21] [link].
URL <http://www.periodictable.com/Properties/A/ShearModulus.html>
- [22] G. Rakhtsaum, Platinum alloys: a selective review of the available literature, *Platinum Metals Rev.* 57 (3) (2013) 202–213. doi:10.1595/147106713X668596.
- [23] G. P. M. Leyson, L. G. Hector Jr., W. A. Curtin, Solute strengthening from first principles and application to aluminum alloys, *Acta Mater.* 60 (9) (2012) 3873 – 3884. doi:http://dx.doi.org/10.1016/j.actamat.2012.03.037.
- [24] G. P. M. Leyson, L. G. Hector Jr., W. A. Curtin, First-principles prediction of yield stress for basal slip in MgAl alloys, *Acta Mater.* 60 (1314) (2012) 5197 – 5203. doi:http://dx.doi.org/10.1016/j.actamat.2012.06.020.